La Rochelle Université

Interanual morphological evolution of an intermediate beach derived from satellite imagery: Cova-Gala, Portugal

Internship report

15/06/2021

par

Jules BUQUEN

Supervisor : Alphonse NAHON
University supervisor : Xavier BERTIN

Laboratório Nacional de Engenharia Civil

LABORATÓRIO NACIONAL
DE ENGENHARIA CIVIL

Table of contents

Abstract

The work presented in this report is a contribution to the MOSAIC.pt project. The project aimed at improving flooding predictions along the continental coast of Portugal. Those predictions are based on a combination of data and numerical model of coastal hydrodynamics. Those models rely on updated topo-bathymetric information, so the present contribution focused on the validation of a method for the recurrent reconstruction of Digital Terrain Models (DTMs) of intertidal areas. The method uses periodical satellite images provided by the WORSICA service. WORSICA builds and gives access to DTM of areas which are intermittently inundated, such as river valleys, estuaries, and, in the present case, intertidal beaches. DTMs are created based on the frequency of inundation over a user-defined period of time. The frequency of inundation is then converted into elevation based on the water level exceedance probability. Here, the images were obtained over a 2-km beach (Cova-Gala) located on the western coast of Portugal, during the summers of 2019, 2020 and 2021. The water level exceedance probability was derived from elevation time series of tidal predictions to which was added the contribution of the atmospheric inverse barometer. Prior to the DTM generation, waterlines were extracted from individual images and converted into topo-bathymetric contours based on the elevation at the fly-over time. These contours were compared to contemporaneous topo-bathymetric data collected with traditional survey methods. In a second step, this comparison was performed for the DTM. It was found that the quality of the DTM improved compared to that of individual waterlines. This explains because the overall frequency of inundation and probability of water level exceedance implicitly filters bias observed for individual waterlines. Thus, the morphologic evolution of the Cova-Gala beach was studied with WORSICA's DTM and compared to the evolution quantified from the reference topo-bathymetric data.

1 Introduction

The Portuguese coast is exposed to flooding due to combined wave-driven overtopping and storm surge [5]. This vulnerability is increasing with sea level rise (SLR). The project MOSAIC.pt aims to develop innovative flood risk management tools based on the integration of predictive models and real-time data. The project is conducted around a scientific question : as the flooding process depends on the characteristics of the exposed territory, how to predict it in the most efficient way and towards the emergency management needs. Three objectives have emerged from this question : 1) to improve flooding prediction for different coastal typologies, 2) to identify coastal typologies affected by flooding, 3) to build tools for emergency response capacity. The present work mainly contribute to the first objective.

For hydrodynamic modelling applications, updated topo-bathymetric of the beach is a key. To get realistic results it is important to have as accurate as possible Digital Terrain Models (DTMs). The “Coastal Monitoring Program of Continental Portugal - COSMO” program was implemented to answer this need. The program consists in the collection, processing and analysis of information on the evolution of beaches, dunes, nearshore seabed and sea cliffs along the Continental Portuguese coast. At Cova-Gala beach, south of Figuera da Foz, harbour in central Portugal, COSMO provides a full topo-bathymetric DTM and an orthophoto every year, based on the data surveyed during the summer. Satellite observation are seen as a means to improve this coverage, in time and also in space. For instance, Satellite Sentinel 2 take an image every 5 days of this area and of the entire Portuguese coast. The aim of the present study was to verify the possibility of using these images to get more frequent topographies of the intertidal beach.

The first objective was to determine the viability of satellite images to get the topography of a given beach. The period of study extent from summer 2019 to summer 2021. To do so, first, two methods to reconstruct the beach topography were tested. The first uses individual waterlines which are associated the elevation at a given instant. The other compiles images over a period of time and build elevations based on a probability of inundation. The following section present the data and the methods. Section 3 present the overall performance of each method in terms of survey accuracy. The discussion focuses on the ability of the second method to follow the observed geomorphological evolution and proposes some way of improving the methods.

2 Methods

2.1 Study area

The study area is the Cova-Gala beach, near Figueira da Foz harbour in central Portugal (Figure 1). It is a sandy beach-dune system with a coastline length approximately 2 kilometres. It is located southern of the south jetty of the Mondego river mouth. Since the last mid-century, the stretch has evolved due to diverse human interventions. Among these, it is important to note that five groynes have been built in 1978-1979 to protect waterfront from coastal erosion. As a results, the beach is divided into different beach cells (Figure 1).

FIGURE 1 – Map displaying each cell and profiles of the study.

2.2 Topographic data and satellite images

The reference topo-bathymetric data used to achieve this project were obtained from the COSMO program and the satellite products were created through the WORSICA service. The "Coastal Monitoring Program of Continental Portugal - COSMO" consists in the collection, processing and analysis of information on the evolution of beaches, dunes, nearshore seabed and sea cliffs along the Continental Portuguese coast. At Cova-Gala, it provides a full DTM and its associated orthophoto once a year in the summer. Here, we used the topo-bathymetric DTMs from summer 2019 to 2021. The DTMs have a resolution 0.3 x 0.3 square meters and cover the full study area. They are given referenced to the chart datum (ZH) and were converted into the national vertical datum in (ALTH38) by removing the official 2.0 m vertical offset. The WORSICA services provides access to satellite images from Copernicus Sentinel-2. Sentinel-2 consists in a constellation of two polar-orbiting satellites placed in the same orbit and are phased 180º from each other. It has a swath width of 290km. Each satellite has a 10-day revisit at the equator leading to a 5-day revisit for the constellation. Here, only the satellite images with less than 10% of cloud coverage were selected. This corresponds to an overall 40 images were used. They were from the months of July and August from 2019 to 2021.

2.3 From NDWI images to topographic images

Sentinel-2 images are composed of twelve bands with resolutions from 10 to 60 meters. Single images were used to extract waterlines at the fly-over time, i.e. the limit between wet and dry areas when the satellite fly over the study area. The waterlines were extracted based on the Normalized Difference Water Index composite images (NDWI ; [6]). The NDWI index is a combination between Band3 (Green,0.560 µm) and Band8 (Near Infrared, 0.842 µm) ; those 2 bands have a 10m resolution. The NDWI combination refers to Equation 1 .

$$NDWI = \frac{Green - NIR}{Green + NIR} \tag{1}$$

Figure 2a) shows an NDWI image for a given Region of Interest (RoI). The water is in light colors and the land in dark colors. The limit between both can either be define as zero, or be scaled based on a threshold value computed from the histogram (Figure 2b). Such an 'auto-threshold' value may be selected in WORSICA, which in either case provides a pixel-sized line (Figure 2). Those lines were first smoothed with the *voronoi.skeleton* function on QGIS (Figure 3), but then the sub-pixel method of Bishop-Taylor et al.(2019) was recovered from the Digital Earth Australia open source code (DEA-tools repository on github). It consists in a python script with the sub-pixel function that was run on the images download from WORSICA. The script evaluates the relative water index of one pixel by comparing it with its neighbour and use this comparison to precise the location of the waterline according to the specified threshold value [2]. The threshold is a key parameter [2]. Results with and without automatic threshold were also be compared. The threshold known, the script, computes and creates the waterline for each image. Then it is possible to add an elevation to the water lines and/or to reconstruct a DTM for a series of images. The water level at flyover time can be linked to extracted waterlines. WORSICA provides tidal level data every 10 minutes. Tidal levels are given with respect to mean sea level and were converted to the national ALTH38 by adding 18 cm to it, according to the data of Antunes [1]. The contribution of the inverse barometer to the total water level was provided by André Fortunato [4] and was added to the tidal level predictions. In 2019, tide

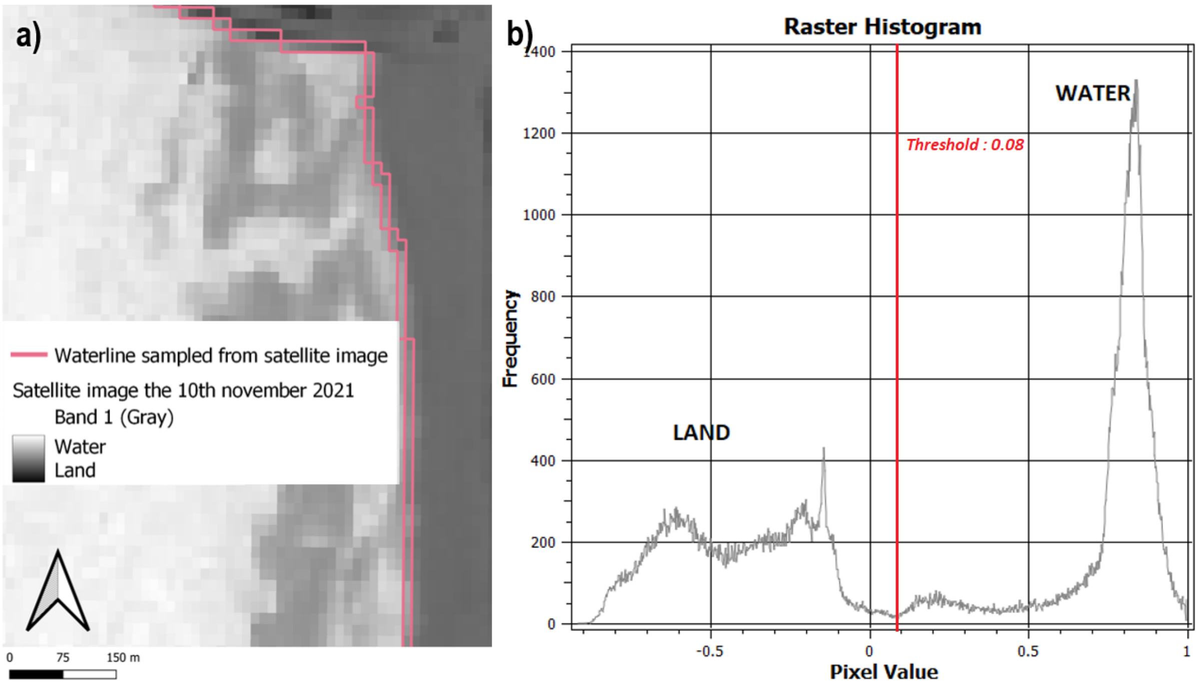

FIGURE 2 – Waterline (a) computed with the auto NDWI threshold (b)

gauge data available for the full year were compared to the reconstruct water level with and without inverse barometer. The tidal gauge record was sampled every hour and was provided by the Portuguese Hydrographic institute for the whole year. The comparison was done resorting to python scripts that were developed for it. For the time being, the contribution of waves (wave induced setup and runup) were not included.

Those time series were used to convert the 2D information from the waterlines into 3D topo-bathymetric contours survey points. The contours were split into 5-meter spaced survey points. To infer on the accuracy of such a surveying method, the COSMO DTMs were sampled onto those points.

2.4 DTM reconstruction

In a second step, DTMs were reconstructed using WORSICA's method. The method consists in using numerous satellite images to compute the flooding frequency [3]. Every time an image is available, it gives flooded and non-flooded areas. By combining every images during a selected period of time, it is possible to know the flooding frequency of every image pixels. A percentage rounded to the nearest ten is given for each pixel (Figure 3). It results in the flooding map. Then the water level for each percentile was computed from the water level exceedance probability computed from the water elevation time series. In the end, it gives a map of water level corresponding to the topography of the beach. Within QGIS, the reconstructed topography was sampled on a regular grid with a 5-meter resolution. The overall spatial data was exported into text files and processed with python scripts to compute the mean (bias) and root means square errors (RMSE) between COSMO and WORSICA's topography year by year. Then, the 'zero' threshold has been compared to the automatic threshold.

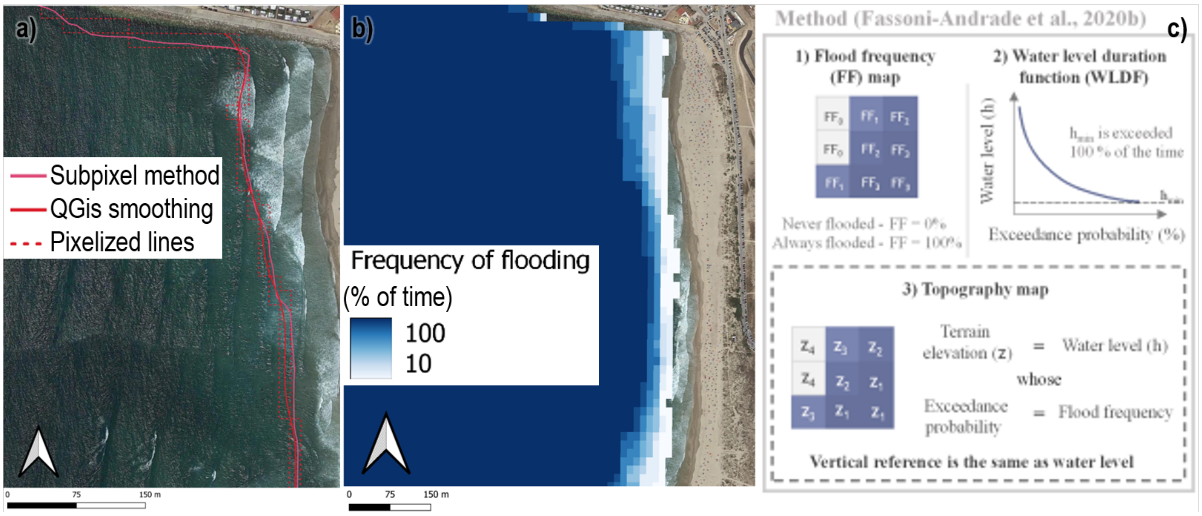

FIGURE 3 – a) The 3 ways of computing a waterline ; b) Flooding frequency map in percentage of time a pixel is flooded ; c) Explanation of the flooding frequency method.

2.5 Bathymetric evolution

The evolution of the beach over two consecutive years was then computed from DTMs obtained with WORSICA and compared to the morphodynamics evolution measured by COSMO. This was done for 2019-2020 and 2020-2021. COSMO and WORSICA interannual evolutions were compared quantitatively and qualitatively. The qualitative analysis was done by resorting to a QGIS plugin (Profile Tool) while the quantitative comparison was made using python script to analyse the spatial data exported from QGIS into text files. To do so, a regular grid with a 5-meter resolution was created. All DTM were sampled onto the grid points. The interanual morphologic evolution was computed at all grid points for both survey methods. The analysis was then subdivided into 5 beach cells. For each cell and for both years pairs of vertical evolution and of the Root Mean Square Evolution were computed based on the sampled grid points. The mean vertical evolution was then normalized by the RMSE for cell. So, if the normalized evolution was below 1, it meant that the data are not usable because the error is greater than the observed evolution. The last parameter checked is the evolution of the volume of sediment by calculating the sum of the difference of each point multiplied by 5 m2 which is the resolution of one point. Ultimately, map of each area has been created which display the range value of Worsica evolution DEM sampled points on the Cosmo evolution DEM.

3 Results

3.1 Individual topographic contours

Figure 4 displays the comparison of the tide gauge data with the reconstructed water levels with the inverse barometer. With and without the inverse barometer, the bias was equal to zero and the RMSE improved from 11 cm to 9 cm by including the inverse barometer. These values are much smaller than the differences observed between COSMO's DTMs and the survey points extracted from the NDWI waterlines. Those differences are summarized on Figure 5 and in Table 1.

Figure 5 displays, for every year, the satellite-derived elevation against the elevation

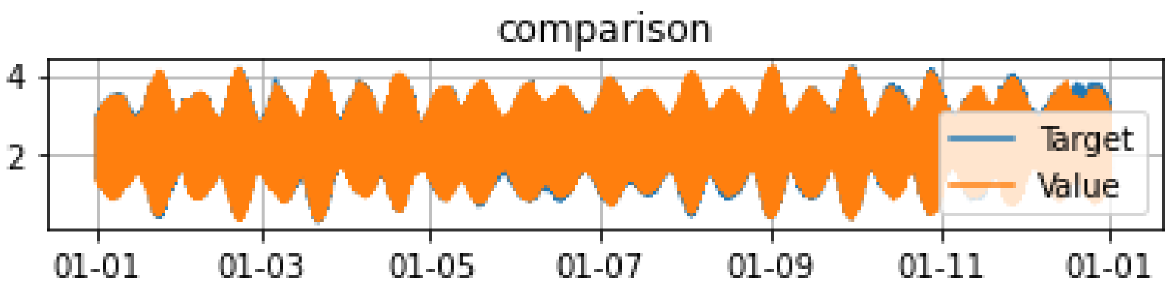

FIGURE 4 – Comparison of the water level computation with in-situ tide gauge with inverted barometer.

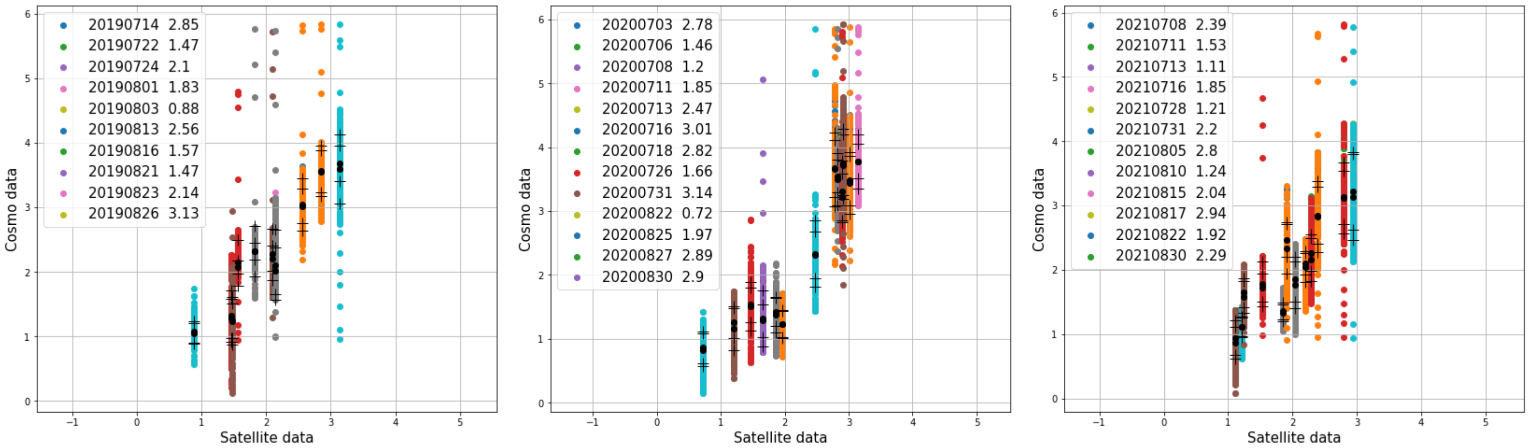

FIGURE 5 – Waterlines water level according to the COSMO sampled value. The mean is represented by a dot (.) and the standard deviation with the crosses (+). 2019 (left), 2020 (center) and 2021 (right).

TABLE 1 – Waterline statistic means by year

Year	Bias	STD	RMS	Bias min	Bias max
2019	-0.351	0.510	0.619	-0.713	0.232
2020	-0.278	0.653	0.709	-0,877	0,734
2021	-0.152	0.484	0.508	-0,410	0,486

from COSMO DEM for every points of the subpixel topographic contours. Each plot displays the mean (dot) and the standard deviation of each contour(+). Individual legends specify the date of acquisition of the satellite images as well as the water elevation at the fly-over time extracted from the reconstructed time series. The vertical dispersion of every set of points suggests there are large uncertainties along every contour. The uncertainty does not appear to the cross-shore position. To check it, for every waterline, the bias, standard deviation and RMSE were computed (Annex A). Yearly means are shown in Table 1. Through the years, the bias, the standard deviation have close values. For every year, the mean bias is negative, ranging from -15 cm to -35 cm. However maximal and minimal values were substantially larger, ranging from -88 cm to + 73 cm. Standard deviation values are around 55 cm and the mean RMSE are in the order of 60 cm +/- 10 cm. An attempt to interpolate these waterlines directly into DTM was made. however, due to to the poor quality of the DTMs, the results were not shown for the time being.

Table 2 – DEM comparison in beach area

Year	Bias	STD	RMSE
2019	0.093	0.273	0.289
2020	0.119	0.335	0.356
2021	0.341	0.447	0.562

3.2 WORSICA's DTM

Table 2 displays the results of the statistical comparison for the northern beach cell (identified as 'beach' on Figure 1).Compared to the mean bias of the individual waterlines, the bias values were always positive. Also, intriguingly, the smaller and larger value were obtained in 2019 and 2020 respectively, which was the opposite in the previous case. It is worst mentioning the DTM creation was relatively effortless, compared to the interpolation of a set of waterlines.

To infer on the possible error due to different type of beaches and the high steepness induced by the groynes, the Cova-Gala beach was divided into 5 cells (Figure 1). Indeed, the results present a large variability between cells (Table 3). Because of this variability, the satellite-derived DTMs were also created without the automatic threshold. To do so, a default zero value was used to distinguished flooded and non-flooded areas when creating the flooding frequency maps.

The 'auto' and 'zero' threshold methods were compared to COSMO DTM, using WORSICA's DMT reconstruction method. Table 3 displays the results.

In eight out of 15 cases, the RMSE values with automatic threshold were lower than with the zero threshold. Also, neither the years or the beach type of the cells appeared to have a specific response depending on the method used. The following comparisons will be computed with the automatic threshold.

3.3 Morphological evolution

The morphological evolution of the northern beach cell ('beach' on Figure 1) is displayed on Figure 6 and summarized in Table B.4 (the table displaying the evolution of the others cells is displayed in Annex 2). Between 2019 and 2020, both COSMO and WORSICA shows an erosion of the beach. The beach evolution between 2019 and 2020 corresponds to a loss of 439 cubic-meters for COSMO and of 183 cubic-meters for WORSICA. Between 2020 and 2021, both DTM have shown an accretion of the beach. The accretion was of 6087 cubic-meters for COSMO and 8245 cubic-meters for WORSICA. Figure 6 describes the spatial variability of the evolution from 2019 to 2020, with eroded areas in grey and accreted area in red. The raster layer shows the morphodynamic of the beach using COSMO's DTM. Using the same color-scale, the dots shows the morphodynamic of the beach using WORSICA's DTM. In this way, the statistical table can be understood qualitatively. Moreover, the figure 6 also displays the COSMO and WORSICA beach profiles trough the years (left) and their difference profiles (center). On profile 11, left plot shows that in 2019, COSMO and WORSICA profiles are close. In 2020 also but a slight gap appears after 180 meters. These proximities are confirmed with the right plot, the difference between 2019 and 2020 shows the same evolution using the 2 sets of DTMs. On the map, the raster and the points are all red, which is confirming the trend of accretion between those 2 summers. On the same area, profile 9 displays a different result. Even if the yearly profile seems quite similar, the evolution is not working as expected.

Table 3 – Table of comparison between automatic and zero threshold for each cell.

BEACH	Zero			Automatic		
	Bias	STD	RMSE	Bias	STD	RMSE
2019	0,204	0,581	0,615	0,197	0,571	0,604
2020	0,136	0,424	0,445	-0,027	0,48	0,481
2021	0,305	0,287	0,419	0,317	0,358	0,478

C0	Zero			Automatic		
	Bias	STD	RMSE	Bias	STD	RMSE
2019	-0,223	0,829	0,859	-0,213	0,787	0,816
2020	0,199	0,479	0,519	0,202	0,372	0,423
2021	0,467	0,286	0,548	0,483	0,377	0,613

C1	Zero			Automatic		
	Bias	STD	RMSE	Bias	STD	RMSE
2019	-0,275	0,356	0,449	-0,283	0,353	0,453
2020	0,122	0,323	0,345	0,073	0,258	0,269
2021	0,503	0,287	0,579	0,478	0,371	0,605

C2	Zero			Automatic		
	Bias	STD	RMSE	Bias	STD	RMSE
2019	0,752	0,531	0,921	0,715	0,531	0,89
2020	-0,034	0,631	0,631	-0,24	0,631	0,675
2021	-0,077	0,656	0,661	-0,339	0,741	0,815

C3	Zero			Automatic		
	Bias	STD	RMSE	Bias	STD	RMSE
2019	-0,101	0,992	0,997	-0,015	0,897	0,897
2020	-0,473	0,612	0,773	-0,446	0,528	0,692
2021	-0,009	0,703	0,703	0,192	0,502	0,537

TABLE 4 – DEM of beach evolution comparison

	WORSICA			COSMO	
	Bias	RMS	NRMS	Bias	RMS
2019-2020	-0.02	0.44	1.36	-0.04	0.43
2020-2021	0.846	1.01	2.19	0.625	0.93

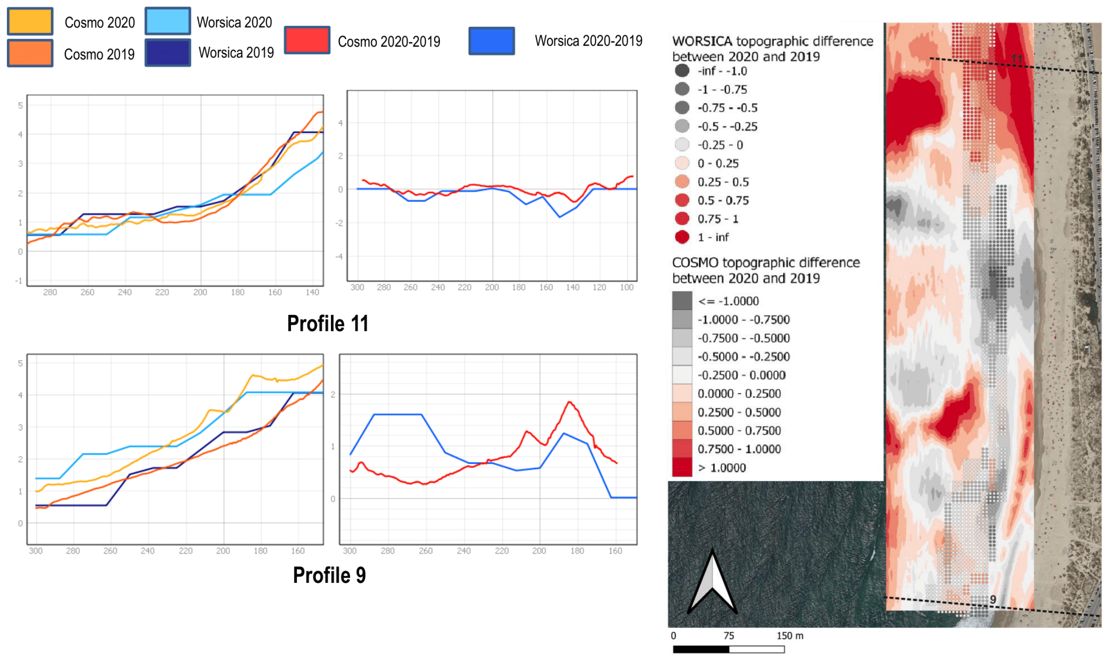

FIGURE 6 – Beach profiles (left) and their evolution (center). On the right, a map displaying the morphological evolution using COSMO overlapped by WORSICA evolution DTM values between 2019 and 2020. Profile 9 down, profile 11 top.

Indeed, the higher part of the studied profile has the same evolution trend, but the lower part does not. Also, on profile 9 on the map, some grey points (erosion) are overlapping red pixels of the raster. In the end, in the Annex 2, some morphodynamic comparison doesn't match. For instance, evolution of C1 are opposite between 2020 and 2021 despite using COSMO (erosion) or WORSICA (accretion).

4 Discussion

4.1 Waterline and full DTM reconstruction comparison

The topographic contours reconstructed from individual images show larger errors than their overall average or than the errors observed from the DTM reconstructed from flooding frequency maps. This may be caused, because the DTM reconstructed filters the variability of the bias as observed in Table 1. Indeed, the overall bias for the survey point extract from the contours, is much lower than the bias of most individual contours. Futhermore, test using or not the 'automatic' threshold were not conclusive in the case of the DTM and may cause higher uncertainty when using a single image. Also, the contribution of waves was not included and may be as well better filtered when using multiple images.

Overall, both method may also suffer additional horizontal errors, due to the pixel resolution and the image georectification, which translate into vertical errors. However, this may not be the dominant contributions as the observed vertical errors did not seem to be affected by the position of the contours across the cross-shore profile. Instead, a interesting finding was that the mean bias of the individual waterlines, was always negative. This may be due to the fact that the contributions (setup and runup) were not taken into account. To dig further on this, a first step would be to compare the errors for the individual contour and the overall means, with respectively the wave height at the fly-over time and its summer average. Also, the mean bias appeared to be somehow compensated when using WORSICA's method. This should be further investigated, for instance looking at results in protected areas to limit the impact of waves.

4.2 Beach morphodynamic

Despite the quantified errors, the study of the beach morphological evolution suggest the method may performed reasonably well in some cases. The most of the cells evolution studied with WORSICA DTM were matching with the COSMO DTMs. Indeed, apart of C0 2020-2021 and C1 2020-2021, every evolutions were going the same direction (i.e., erosion or accretion), even if the values can be distant. For instance, the Normalized Root Mean Square evolutions in Table B.4 (NRMS, RMS values normalized by the errors associated to each DTM in Table 2, indicate the morphological variability of the study area is larger than the reconstruction method. Indeed, those values are higher. In 2020-2021, C0 and C1 had respectively 58 cm and 66 cm difference between COSMO and WORSICA difference, and both had inverse evolution. These errors can be explained with the mean RMS between 2020 and 2021 for each cell which were respectively of 67 cm and 52 cm. In the end, even if the evolution trend can be computed with satellite images, the vertical error seems to be too important to survey a beach morphodynamic only with this method. A better resolution and a lower revisiting time could help to get better results. The first would reduce the error and may permit the use of the individual waterlines. The second could help getting more images with an acceptable cloud coverage.

5 Conclusion

During the over all 6-week internship period, at range of QGis and Python tools were used to process geomorphological and water level data with the objective to evaluate the quality of topo-bathymetric products derived from satellite images. These tools include the model builder functions for routinely extracting information from raster layers and exported into formatted text files. The Python script were developed to compute errors associated with the different surveying processes. A significant amount of data was downloaded from data repositories and created with the WORSICA on-line service. The comparison of this data showed that the satellite images may be used to easily create initial topo-bathymetric conditions for hydrodynamic models. However, some improvements should be achieved to use this information as a recurrent update to the model DTMs. For instance, the impact of wave should taken into account and improve the DTMs. Also, some spatial interpolation techniques should be further tested.

Bibliography

[1] Antunes, C. (2019). Assessment of Sea Level Rise at West Coast of Portugal Mainland and Its Projection for the 21st Century. J. Mar. Sci. Eng. Int., 7(3), 61, doi.org/10.3390/jmse7030061

[2] Bishop-Taylor, Robbi, Stephen Sagar, Leo Lymburner, Imam Alam, and Joshua Sixsmith. "Sub-Pixel Waterline Extraction : Characterising Accuracy and Sensitivity to Indices and Spectra." Remote Sensing 11, no. 24 (January 2019) : 2984. https ://-doi.org/10.3390/rs11242984.

[3] Fassoni-Andrade, Alice César, Fabien Durand, Daniel Moreira, Alberto Azevedo, Valdenira Ferreira dos Santos, Claudia Funi, and Alain Laraque. "Comprehensive Bathymetry and Intertidal Topography of the Amazon Estuary." Earth System Science Data 13, no. 5 (May 26, 2021) : 2275–91. https ://doi.org/10.5194/essd-13-2275-2021.

[4] Fortunato, A.B., Meredith, E.P., Rodrigues, M. et al. Near-future changes in storm surges along the Atlantic Iberian coast. Nat Hazards 98, 1003–1020 (2019). https ://doi.org/10.1007/s11069-018-3375-z

[5] Freire, P., F.S.B.F. Oliveira, J.N.C. Oliveira, 2020. Coastal flooding process : comparing different coastal typologies response to extreme hydrodynamic conditions. J. Coast. Res., SI 95 : 797-802.

[6] McFeeters, S. K. "The Use of the Normalized Difference Water Index (NDWI) in the Delineation of Open Water Features." International Journal of Remote Sensing 17, no. 7 (May 1996) : 1425–32. https ://doi.org/10.1080/01431169608948714.

[7] Otsu, Nobuyuki. "A Threshold Selection Method from Gray-Level Histograms." IEEE Transactions on Systems, Man, and Cybernetics 9, no. 1 (January 1979) : 62–66. https ://doi.org/10.1109/TSMC.1979.4310076.

[8] Fangfang Zhang, Junsheng Li, Bing Zhang, Qian Shen, Huping Ye, Shenglei Wang, Zoe lu, 2018. A simple automated dynamic threshold extraction method for the classification of large water bodies from landsat-8 OLI water index images. International Journal of Remote Sensing, 39(11) :3429-3451. DOI : 10.1080/01431161.2018.1444292

Annexe A

Table A.1 – 2019

Date	Bias	STD	RMSE
2019/07/14	-0.713	0.392	0.814
2019/07/22	0.145	0.395	0.421
2019/07/24	-0.173	0.399	0.435
2019/08/01	-0.496	0.392	0.633
2019/08/03	-0.192	0.165	0.253
2019/08/13	-0.486	0.406	0.633
2019/08/16	-0.575	0.358	0.678
2019/08/21	0.232	0.370	0.436
2019/08/23	0.032	0.543	0.544
2019/08/26	-0.464	0.540	0.712
MEAN	-0.351	0.510	0.619

Table A.2 – 2020

Date	Bias	STD	RMSE
2020/07/03	-0,877	0,574	1,048
2020/07/06	-0,046	0,377	0,380
2020/07/08	0,050	0,329	0,332
2020/07/11	0,480	0,275	0,553
2020/07/13	0,136	0,520	0,538
2020/07/16	-0,427	0,477	0,640
2020/07/26	0,336	0,439	0,553
2020/07/28	-0,638	0,426	0,767
2020/07/31	-0,675	0,415	0,792
2020/08/18	-0,110	0,254	0,277
2020/08/22	0,734	0,211	0,764
2020/08/25	-0,422	0,483	0,641
2020/08/27	-0,842	0,548	1,005
2020/08/30	-0,439	0,556	0,708
MEAN	-0.278	0.653	0.709

Table A.3 – 2021

Date	Bias	STD	RMSE
2021/07/08	-0,249	0,350	0,430
2021/07/11	0,162	0,273	0,317
2021/07/13	0,486	0,130	0,503
2021/07/16	0,096	0,151	0,179
2021/07/26	0,167	0,227	0,282
2021/07/28	-0,319	0,548	0,635
2021/07/31	-0,336	0,245	0,416
2021/08/05	0,273	0,357	0,450
2021/08/10	-0,196	0,668	0,696
2021/08/15	-0,410	0,379	0,559
2021/08/17	0,133	0,330	0,356
MEAN	-0.152	0.484	0.508

Annexe B

Table B.1 – DEM of C0 evolution comparison

	WORSICA			COSMO	
	Bias	RMS	NRMS	Bias	RMS
2019-2020	0.586	0.757	1.51	0.597	1.1
2020-2021	0.4	0.568	0.85	-0.182	0.636

Table B.2 – DEM of C1 evolution comparison

	WORSICA			COSMO	
	Bias	RMS	NRMS	Bias	RMS
2019-2020	0.451	0.641	1.303	0.888	1.18
2020-2021	0.349	0.557	1.07	-0.307	0.427

Table B.3 – DEM of C2 evolution comparison

	WORSICA			COSMO	
	Bias	RMS	NRMS	Bias	RMS
2019-2020	-0.648	0.695	1.04	-0.617	0.686
2020-2021	-0.381	0.516	0.69	-0.99	1.05

Table B.4 – DEM of C3 evolution comparison

	WORSICA			COSMO	
	Bias	RMS	NRMS	Bias	RMS
2019-2020	-0.239	0.573	0.52	-0.145	0.931
2020-2021	-0.657	0.741	0.73	-1.43	1.5